Supplementary Information

Direct printing of high-performance micro-supercapacitors on flexible substrates using polymeric stencil masks with highly precise interdigitated patterns

Kwang-dong Seong,[1] Jae-Yeong Jung,[2] Jeongmin Kang,[1] Da-Seul Kim,[2] Lulu Lyu,[1] Soonmin Seo,[3,*] Ju-Hyung Kim[2,4,*] and Yuanzhe Piao[1,5,*]

[1]Program in Nano Science and Technology, Graduate School of Convergence Science and Technology, Seoul National University, 145 Gwanggyo-ro, Yeongtong-gu, Suwon 16229, Republic of Korea

[2]Department of Energy Systems Research, Ajou University, 206 Worldcup-ro, Yeongtong-gu, Suwon 16499, Republic of Korea

[3]College of BioNano Technology, Gachon University, 1342 Seongnamdaero, Sujeong-gu, Seongnam 13120, Republic of Korea

[4]Department of Chemical Engineering, Ajou University, 206 Worldcup-ro, Yeongtong-gu, Suwon 16499, Republic of Korea

[5]Advanced Institutes of Convergence Technology, 145 Gwanggyo-ro, Yeongtong-gu, Suwon 16229, Republic of Korea

[*]Correspondence and requests for materials should be addressed to S.S. (email: soonmseo@gachon.ac.kr), J.-H.K. (email: juhyungkim@ajou.ac.kr) and Y.P. (email: parkat9@snu.ac.kr).

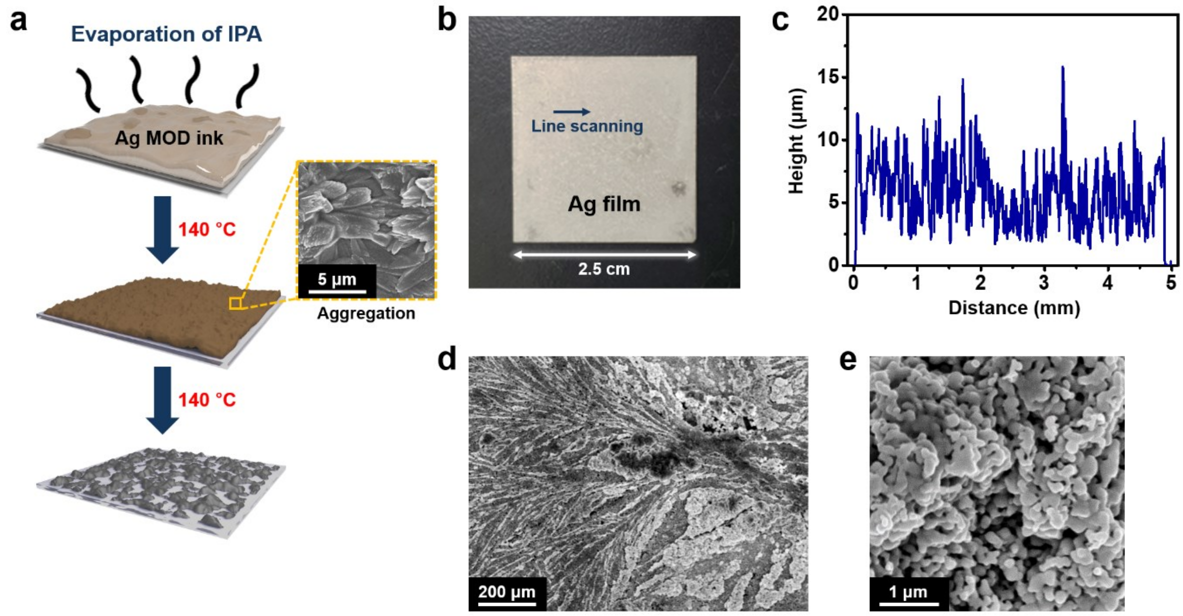

Figure S1. (a) Schematic illustration of the Ag film formation by drop-casting of the Ag MOD ink. (b) Photograph of the Ag film prepared as in (a). (c) The height profile along the blue arrow in (b). (d) SEM image of the Ag film prepared as in (a). (e) Close-up SEM image of (d).

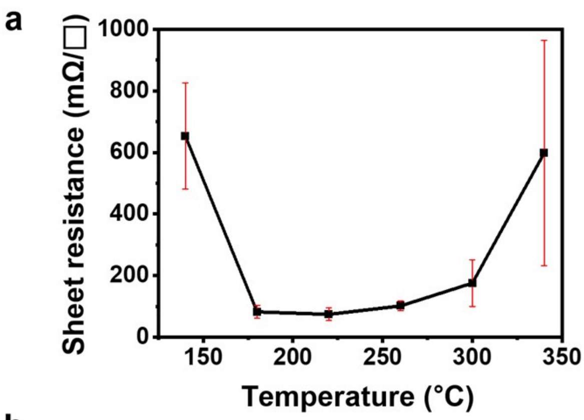

Temperature (°C)	Sheet resistance (mΩ/□)	Standard deviation (mΩ/□)	Resistivity (μΩ cm)
140	653.5	172.3	78.4
180	82.5	21.0	9.9
220	75.5	20.4	8.9
260	101.9	15.9	12.2
300	176.0	75.6	21.1
340	597.9	366.0	71.8

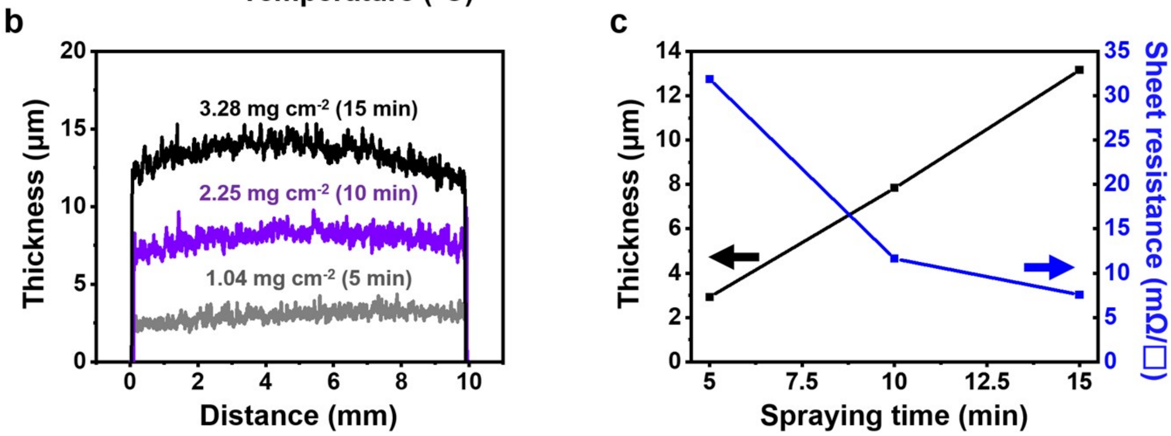

Figure S2. (a) Sheet resistance of the printed Ag film according to the processing temperature. Standard deviations are indicated by vertical red bars. (b) Thickness profile and loading mass of the printed Ag film according to the spraying time. (c) Thickness and sheet resistance of the printed Ag film at the optimal condition, according to the spraying time. The overall resistivity was consistently maintained at ~9 μΩ cm, regardless of the film thickness.

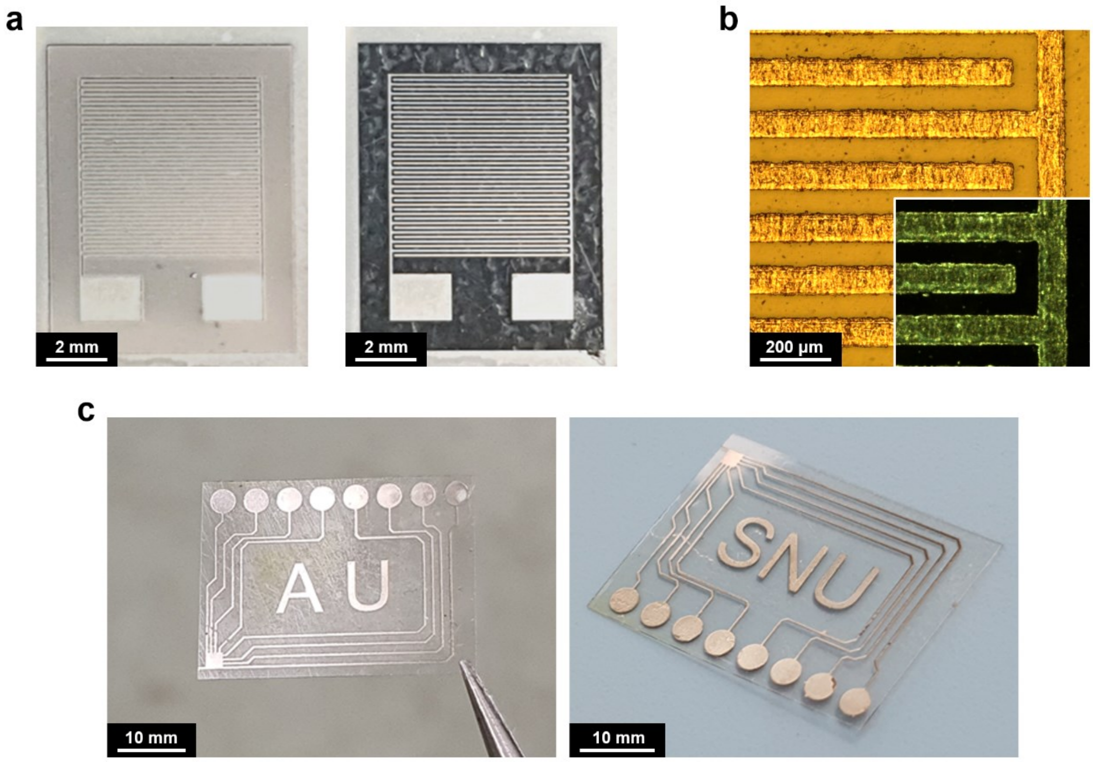

Figure S3. (a) Photographs of the printed Ag electrodes on the flexible PET substrate, of which both electrode and gap widths are 75 μm, before (left) and after (right) peeling off the PUA mask. (b) Optical microscopy image of the same sample as in (a). Inset is the corresponding dark-field microscopy image, exhibiting the light scattered by the metallic Ag film. (c) Photographs of exemplary Ag patterns for electronic circuits, printed on the flexible PET substrates.

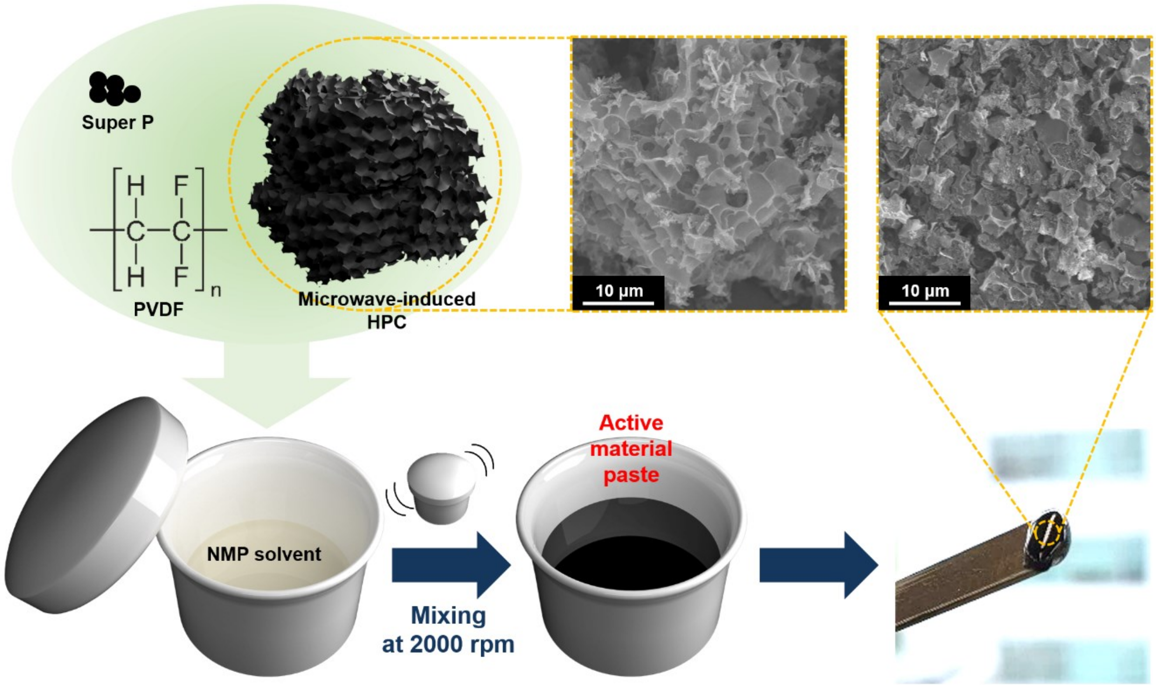

Figure S4. Schematic diagram showing the preparation of active material paste.

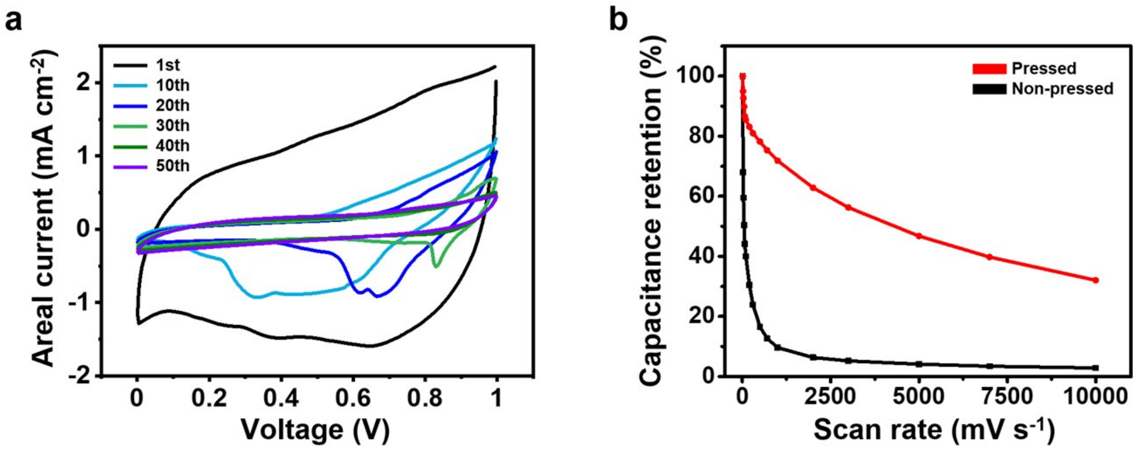

Figure S5. (a) Current-versus-voltage (I–V) characteristics of the printed MSC (500-μm-resolution without the roll-pressing process), corresponding to 50 cycle measurements. It was found that a large amount of the active material was peeled off within the 50 cycles. (b) Capacitance retention of the printed MSCs (500-μm-resolution with and without the roll-pressing process) after 100 cycle measurements.

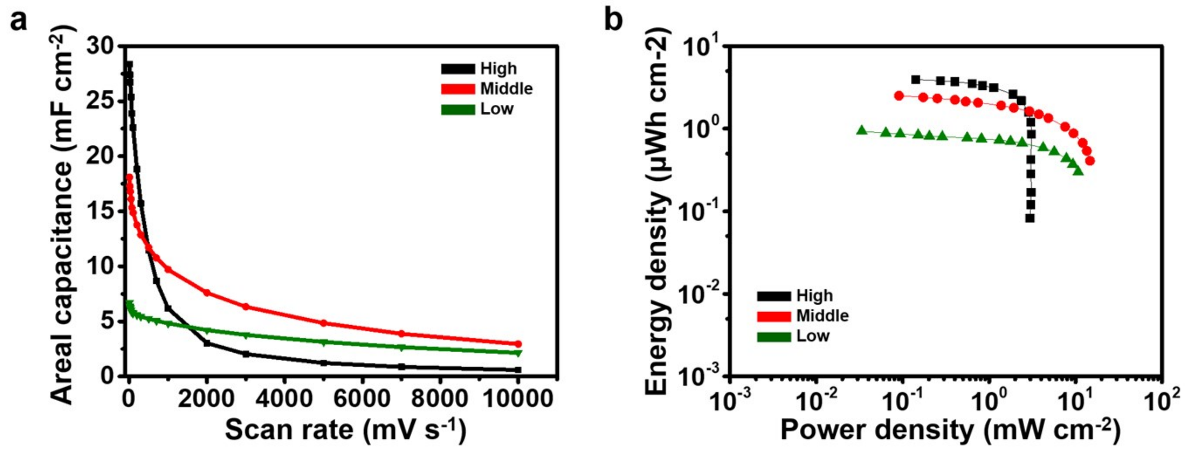

Figure S6. (a) Electrochemical performances of the printed MSCs with varied thicknesses of the active layers. The height of the PUA mask was adjusted to change the thickness of the active layer, and the 500-μm-resolution pattern was used to clarify the difference in loading amount of the active material for each MSC. In complete device configuration, the thicknesses of the active layers were measured to be ~9, ~14, and ~19 μm for low, middle, and high loads, respectively. (b) The Ragone plots of the printed MSCs as presented in (a).

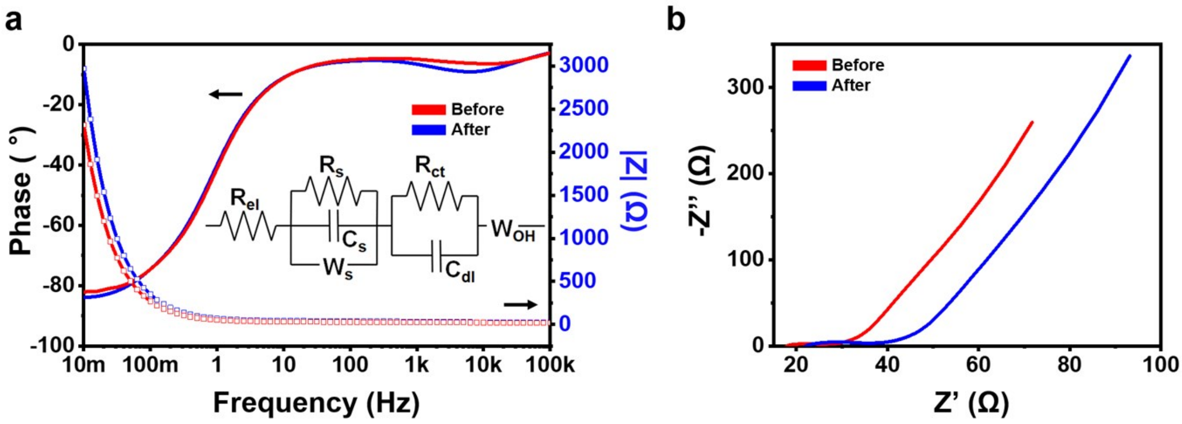

c

	Before	After
Electrolyte-electrode resistance (R_{el})	17.85 Ω	21.99 Ω
Charge transfer resistance (R_{ct})	9.98 Ω	16.01 Ω
Surface resistance (R_s)	13.30 kΩ	59.79 kΩ
Bulk diffusion impedance (W_{OH})	23.86 mΩ	17.73 mΩ
Surface layer diffusion impedance (W_s)	582.90 μΩ	379.24 μΩ
Surface layer geometrical capacitance (C_s)	564.13 nF	909.88 nF
Double layer capacitance (C_{dl})	7.15 mF	5.60 mF

Figure S7. (a) Bode plots of the printed MSC with the 75-μm-resolution pattern before and after 15,000 charges/discharge cycles, corresponding to a frequency range of 10 mHz to 100 kHz with an amplitude of 10 mV at the open-circuit potential. The equivalent circuit is shown in inset. (b) Nyquist plots of (a) for the whole range. (c) EIS fitted parameters of (a).

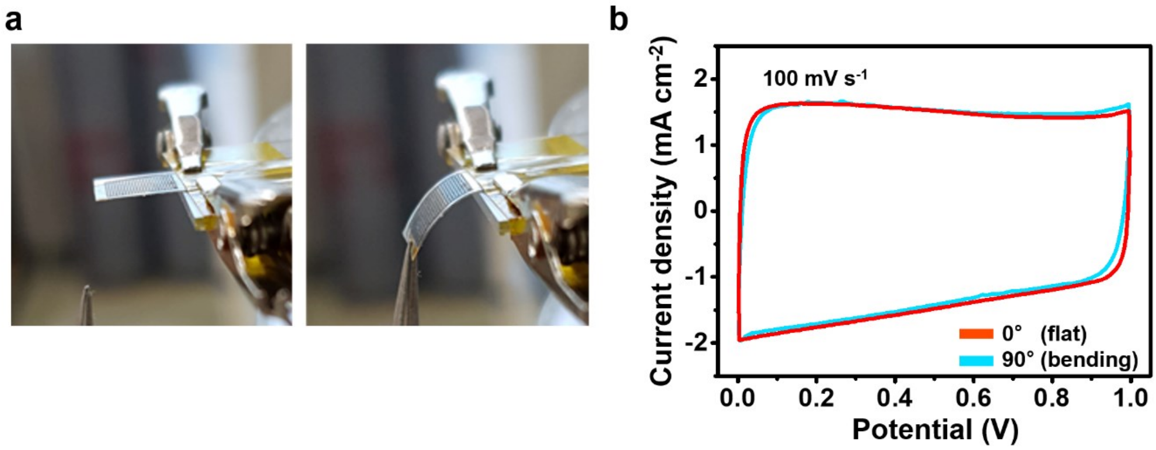

Figure S8. (a) Photographs of the printed MSC, corresponding to the elastic banding of the flexible PET substrate. (b) CV curves of the printed MSC with the 75-μm-resolution pattern in response to the elastic banding of the flexible PET substrate (with a bending radius of 6 mm, and a bending angle of 90°).

Table S1. Characteristics of printed MSCs presented in this work (with the 75-μm-resolution pattern) and other recent reports.

Material	Method	Resolution [μm]	Areal capacitance [mF cm^{-2}]	Voltage [V] (electrolyte)	Energy density [μWh cm^{-2}] @ power density [mW cm^{-2}]	Ref.*
HPC/Ag	Spray/blade printing	75	19.4 @ 10 mV s^{-1}	1 (KOH/PVA)	2.7 @ 0.1, 1.17 @ 42.3	This work
ECG/SWCNTs/Ag	Screen printing	800	7.7 @ 5 mV s^{-1}	1 (H_3PO_4/PVA)	1.07 @ 0.02 0.014 @ 0.32	21
$Ti_3C_2T_x$	Extrusion printing	89	9.2 @ 0.02 mA cm^{-2}	0.5 (H_2SO_4/PVA)	0.32 @ 0.011, 0.11 @ 0.158	32
	Inkjet printing	80	3 @ 0.02 mA cm^{-2}	0.5 (H_2SO_4/PVA)	Not available	
RuO2/AgNW/rGO	Screen printing	200	26 @ 1 mV s^{-1}	1 (KOH/PVA)	3.6 @ 0.013 0.625 @ 3.375	33
Graphene /SWCNT	Screen printing	600	1.324 @ 0.015 mA cm^{-2}	1.8 (H_2PO_4/PVA)	0.55 @ 0.012, 0.064 @ 20.13	34
Graphene	Screen printing	1,000	1.04 @ 10 mV s^{-1}	0.8 (H_3PO_4/PVA)	0.09 @ 0.004, 0.052 @ 0.116	35
$TTi_3C_2T_x$	Screen printing	200	39.5 @ 0.08 mA cm^{-2}	0.6 (H_2PO_4/PVA)	1.64 @ 0.02, 1.15 @ 1.15	36
$Ti_3C_2T_x$	Stamping (contact printing)	550	5 @ 0.8 mA cm^{-2}	0.6 (H_2SO_4/PVA)	0.76 @ 0.006, 0.63 @ 0.33	37
3DGN/SWNT/ AgNW/Graphite	Plotter cutting	500	19 @ 0.01 mA cm^{-2}	1 (LiCl/PVA)	2.75 @ 0.0057, 0.1 @ 0.361	38

*References (cited in the main text)

21 J. K. Chih, A. Jamaluddin, F. Chen, J. K. Chang and C. Y. Su, *J. Mater. Chem. A*, 2019, **7**, 12779-12789.

32 C. (J.) Zhang, L. McKeon, M. P. Kremer, S.-H. Park, O. Ronan, A. Seral-Ascaso, S. Barwich, C. Ó. Coileáin, N. McEvoy, H. C. Nerl, B. Anasori, J. N. Coleman, Y. Gogotsi and V. Nicolosi, *Nat. Commun.*, 2019, **10**, 1795.

33 H. Li, S. Liu, X. Li, Z.-S. Wu and J. Liang, *Mater. Chem. Front.*, 2019, **3**, 626-635.

34 S. Bellani, E. Petroni, A. E. Del Rio Castillo, N. Curreli, B. Martín-García, R. Oropesa-Nuñez, M. Prato and F. Bonaccorso, *Adv. Funct. Mater.*, 2019, **29**, 1807659.

35 X. Shi, S. Pei, F. Zhou, W. Ren, H.-M. Cheng, Z.-S. Wu and X. Bao, *Energy Environ. Sci.*, 2019, **12**, 1534-1541.

36 S. Abdolhosseinzadeh, R. Schneider, A. Verma, J. Heier, F. Nüesch and C. (J.) Zhang, *Adv. Mater.*, 2020, **32**, 2000716.

37 C. (J.) Zhang, M. P. Kremer, A. Seral-Ascaso, S.-H. Park, N. McEvoy, B. Anasori, Y. Gogotsi and V. Nicolosi, *Adv. Funct. Mater.*, 2018, **28**, 1705506.

38 S.-W. Kim, K.-N. Kang, J.-W. Min and J.-H. Jang, *Nano Energy*, 2018, **50**, 410-416.

Electrochemical Characterization

A CHI 660 electrochemical workstation was used to measure the electrochemical performance. The total areal capacitance of the MSC was calculated using the following equation:

$$C_a = \frac{\int I(V)\,dV}{v\,A\,\Delta V}$$

where C_a is the areal capacitance (F cm^{-2}), I(V) is the voltammetric discharge current (mA), v is scan rate (mV s^{-1}), A is the total area (cm^{-2}), and ΔV is the potential range (V). The areal capacitance per electrode can be obtained by multiplying this equation by 4.

The following equations were used to calculate the areal energy and power densities of the MSC:

$$E_a = \frac{0.5\,C_a\,\Delta V^2}{3600}$$

$$P_a = \frac{3.6\,E_a\,v}{\Delta V}$$

where E_a is the areal energy density (Wh cm^{-2}), and P_a is the areal power density (W cm^{-2}).